Geophysical Journal International

Geophys. J. Int. (2015) **202,** 993–1004
GJI Geodynamics and tectonics

doi: 10.1093/gji/ggv200

New Insights into the present-day kinematics of the central and western Papua New Guinea from GPS

A. Koulali,[1] P. Tregoning,[1] S. McClusky,[1] R. Stanaway,[2] L. Wallace[3] and G. Lister[1]

[1] *Research School of Earth Sciences, Australian National University, Canberra ACT* 0200, *Australia. E-mail: achraf.koulali@anu.edu.au*
[2] *School of Civil and Environmental Engineering, University of New South Wales, Australia*
[3] *Institute for Geophysics, University of Texas at Austin, Austin, TX, USA*

Accepted 2015 May 12. Received 2015 March 4; in original form 2014 August 7

SUMMARY

New Guinea is a region characterized by rapid oblique convergence between the Pacific and Australian tectonic plates. The detailed tectonics of the region, including the partitioning of relative block motions and fault slip rates within this complex boundary plate boundary zone are still not well understood. In this study, we quantify the distribution of the deformation throughout the central and western parts of Papua New Guinea (PNG) using 20 yr of GPS data (1993–2014). We use an elastic block model to invert the regional GPS velocities as well as earthquake slip vectors for the location and rotation rates of microplate Euler poles as well as fault slip parameters in the region. Convergence between the Pacific and the Australian plates is accommodated in northwestern PNG largely by the New Guinea Trench with rates exceeding 90 mm yr^{-1}, indicating that this is the major active interplate boundary. However, some convergent deformation is partitioned into a shear component with ∼12 per cent accommodated by the Bewani-Torricelli fault zone and the southern Highlands Fold-and-Thrust Belt. New GPS velocities in the eastern New Guinea Highlands region have led to the identification of the New Guinea Highlands and the Papuan Peninsula being distinctly different blocks, separated by a boundary through the Aure Fold-and-Thrust Belt complex which accommodates an estimated 4–5 mm yr^{-1} of left-lateral and 2–3 mm yr^{-1} of convergent motion. This implies that the Highlands Block is rotating in a clockwise direction relative to the rigid Australian Plate, consistent with the observed transition to left-lateral strike-slip regime observed in western New Guinea Highlands. We find a better fit of our block model to the observed velocities when assigning the current active boundary between the Papuan Peninsula and the South Bismark Block to be to the north of the city of Lae on the Gain Thrust, rather than on the more southerly Ramu-Markham fault as previously thought. This may indicate a temporary shift of activity onto out of sequence thrusts like the Gain Thrust as opposed to the main frontal thrust (the Ramu-Markham fault). In addition, we show that the southern Highlands Fold-and-Thrust Belt is the major boundary between the rigid Australian Plate and the New Guinea Highlands Block, with convergence occurring at rates between ∼6 and 13 mm yr^{-1}.

Key words: Seismic cycle; Plate motions; Continental margins: convergent; High strain deformation zones; Crustal structure; Pacific Ocean.

1 INTRODUCTION

Papua New Guinea (PNG) is one of the most tectonically complex regions in the world, involving microblocks rotating rapidly about nearby poles. The general tectonic framework of this region (Fig. 1) has been related to the southwest-northeast convergence between the Australian and Pacific plates at ∼110 mm yr^{-1} (Johnson & Molnar 1972; DeMets *et al.* 1994; Tregoning *et al.* 1998), implying a convergence of more than 70 mm yr^{-1} across the PNG land mass (Tregoning *et al.* 1998; Tregoning & Gorbatov 2004). This zone of convergence is characterized by a variety of plate boundary types including subduction zones (New Guinea and New Britain Trenches), rifting (Woodlark), collision orogenesis (Finisterre Arc collision, and the New Guinea Highlands) and a strike-slip transform system (Bismarck Sea Seismic Lineation, BSSL; Fig. 1). The kinematics and the partitioning of deformation within this zone are still widely debated. For example, it has been considered that the southern parts of the New Guinea Highlands are stable areas of the northern rigid Australian Plate (Hamilton 1979); however, the spatial extent of the boundary separating the Australian Plate

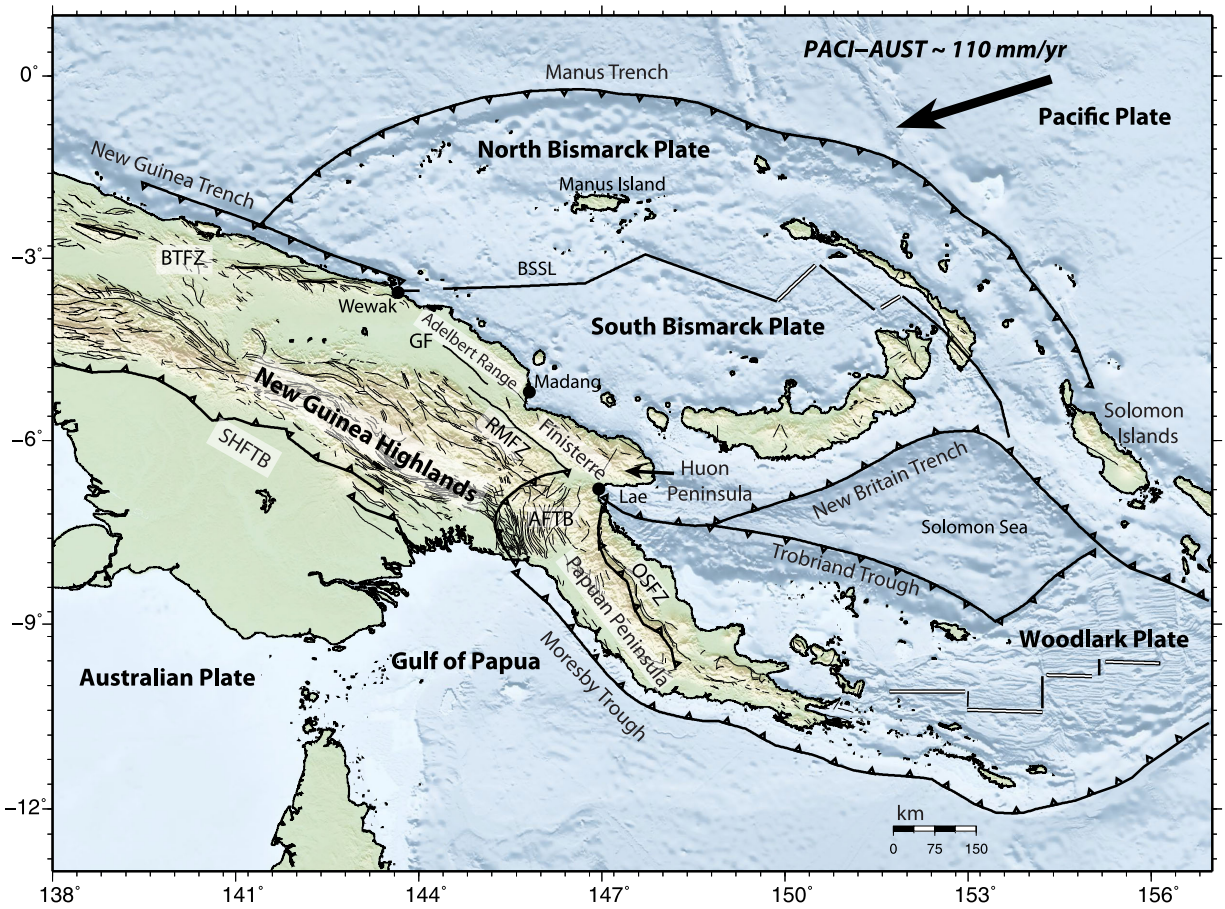

Figure 1. Tectonic setting of the Papua New Guinea region. Topography and bathymetry are from SRTM (http://topex.ucsd.edu/www_html/srtm30_plus.html). Faults are mostly from the East and Southeast Asia (CCOP) 1:2000000 geological map (downloaded from http://www.orrbodies.com/resources/item/orr0052). AFTB, Aure Fold-and-Thrust Belt; OSZF, Owen Stainly fault zone; GF, Gogol fault; BTFZ, Bewani-Torricelli fault zone; RMFZ, Ramu-Markham fault zone; BSSL, Bismarck Sea Seismic Lineation.

from the New Guinea Highlands Block has never been uniquely identified. Wallace *et al.* (2004) described the New Guinea Highlands as a single block extending in a northwest-southeast direction from the New Guinea Trench to the Owen Stanley Range bounding the Woodlark microplate and suggested that the central part of the New Guinea Highlands is rotating as a rigid block. The sparsity of Wallace *et al.*'s (2004) GPS network in the Highlands made it difficult for them to determine where the boundaries of the New Guinea Highlands block are, and how far west it continues.

Plate convergence obliquity has been suggested as one of the factors causing the partitioning of deformation in subduction zones by increasing the amount of shear stress present in the overriding plate (McCaffrey 1992, 1996). In the context of subduction zones, the total slip may be partitioned into shear and thrust components, which are accommodated on different structural components. The New Guinea Trench is an example of such a structure that accommodates oblique convergence between the Pacific and the New Guinea Highlands, but the precise partitioning of the activity across this boundary has been widely debated. Based on seismic tomography and locations of recent thrust events, Tregoning & Gorbatov (2004) concluded that the New Guinea Trench is an active interplate boundary accommodating convergence specifically along the Wewak segment. However, the obliquity of Pacific/Australia convergence at the New Guinea Trench begs the question of how much of the strike-slip component is accommodated in the upper plate, as is observed at other obliquely convergent plate boundaries (McCaffrey 1992, 1996). In northwest PNG, the primary candidate for strike-slip in the upper plate is within the Bewani-Toricelli ranges (Fig. 1).

In this paper, we present an updated GPS velocity field including new data from 1993 to 2014. We use the new velocity field together with velocities along the colliding Finisterre arc (Wallace *et al.* 2004) to assess the kinematics of plate boundaries in western and central PNG extending from the New Guinea Trench to the northern margin of the Australian Plate in the south. We use the combined GPS velocity field to constrain an elastic block model whose bounding fault geometry is based on available geologic and seismic data to understand the tectonic relationships and the dynamics of the deformation in PNG.

2 TECTONIC SETTING OF PAPUA NEW GUINEA

The tectonic setting of the PNG region is associated with the interaction of four of the Earth's major and highly dynamic lithospheric plates: the Australian, Pacific, Philippine Sea and Sunda plates (Bird 2003; Hill *et al.* 2003). The tectonic evolution of the New Guinea region has been dominated by the convergence of the Australian (AUST) and Pacific (PACI) plates since the Cenozoic, resulting in a series of successive collisions (Johnson & Molnar 1972; Davies *et al.* 1987). In northwestern New Guinea, the main

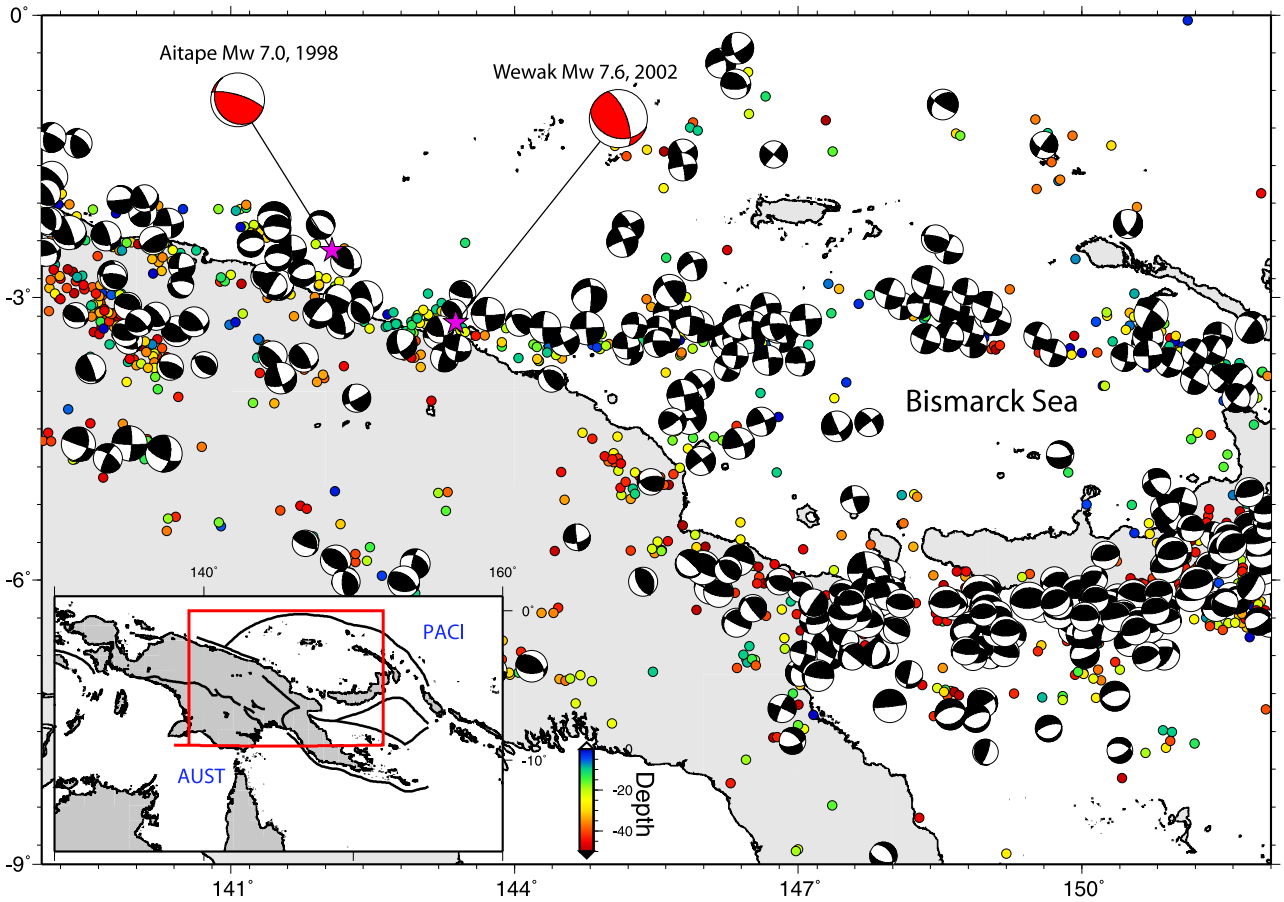

Figure 2. Focal mechanism for earthquakes, from the Global CMT catalogue, with Mw > 5.5 and depth less than 100 km. Seismicity is from ISC Bulletin with magnitudes more than 4.8 and depth between 0 and 60 km depth (1964 to April 2012).

structural units accommodating the AUST–PACI convergence are the left-lateral strike-slip motion on an E-W fault system associated with the BSSL and the New Guinea Trench, where the Pacific Plate subducts beneath continental PNG (Fig. 1). Further to the east, the Ramu-Markham fault zone (RMFZ) and the New Britain Trench form the boundary separating the New Guinea Highlands and the Papuan Peninsula from the South Bismarck Plate. The latter formed in the Late Miocene when the Finisterre volcanic arc collided with the New Guinea land mass, rapidly uplifting the Finisterre Ranges and Huon Peninsula (Abbott *et al.* 1994b). This southeastward propagating collision has been related to the closure of the Solomon Sea (Abbott *et al.* 1994a).

Seismological studies of the region (Abers & McCaffrey 1994; Pegler *et al.* 1995) delineate many major features related to New Britain Trench Wadati-Benioff zone. The southern Highlands Fold-and-Thrust belt shallow events mark the boundary of collisional orogenesis (Abers & McCaffrey 1988; Fig. 2). Large, shallow earthquakes located beneath the Finisterre Ranges were attributed to the north dipping ramp-detachment thrust system of the Ramu-Markham valley (Stevens *et al.* 1998). Fig. 2 shows a northeast trending zone of shallow strike-slip events north of Madang and south of the Adelbert Ranges. Abers & McCaffrey (1988) suggested that this structure is related to many strike-slip events dividing the Huon Peninsula-Finisterre Ranges into small blocks rotating in a clockwise direction. Previous GPS results were inconclusive with respect to this hypothesis (Wallace *et al.* 2004).

The largest earthquakes in our study area have occurred in the northern coastal region of the New Guinea and are associated with ongoing subduction at the New Guinea Trench (Okal 1999). Many of these earthquakes generated devastating tsunamis, such as the Aitape Earthquake (Mw 7.0; 141.926°E) in 1998 and the Mw 7.6 earthquake that occurred on 8 September 2002 near Wewak (142.870°E) (Davies *et al.* 2002; Borrero *et al.* 2003). Most earthquake focal mechanisms available for this region are indicative of thrust events, which argues for the existence of active oblique subduction beneath the north coast of New Guinea.

Previous GPS studies in PNG (McClusky *et al.* 1994; Stevens *et al.* 1998; Tregoning *et al.* 1998; Tregoning *et al.* 1999; Wallace *et al.* 2004) have quantified the horizontal velocity field. Tregoning *et al.* (1998) presented a velocity field from 20 stations well distributed over the New Guinean region, observed over 5 yr. They suggested a plate tectonic model including, in addition to the Australian and Pacific plates, the Solomon Sea Plate, the South Bismarck Plate, the Woodlark Plate as well as an additional North Bismarck Plate. Wallace *et al.* (2004) expanded the PNG network with an additional 35 stations covering the major part of the Finisterre arc-continent collision and continuing into parts of the New Guinea Highlands. They presented a model of six blocks, including the previously defined five blocks of Tregoning *et al.* (1998) plus a New Guinea Highland block. They suggested that edge forces, initiated by the collision between the Finisterre Arc and the New Guinea Highlands, control the rapid clockwise rotation of the South Bismarck Plate. Based on a block model constrained with GPS velocities and earthquake slip vectors, they also quantified the slip-deficit along the Ramu-Markham fault and found that large portions of this fault are locked, accommodating up to 61 mm yr^{-1} of convergence

between the New Guinea Highlands and Australian plates. However, the convergence pattern and rate in the plate boundary zone to the Northwest of the Finisterre collision has not been studied due to the lack of GPS observations.

3 GPS OBSERVATIONS AND ANALYSIS

3.1 Data processing

Our GPS velocity field is derived from data collected at GPS sites from 1993 to 2014. We have reprocessed GPS data collected between 1993 and 1999 and added new observations from 2000 until 2014. Most of the sites were observed with Ashtech ZXII and Trimble 4000SSI receivers and choke-ring antennas and were occupied at least 2 d yr^{-1} during the data collection period. We have used 36 campaign stations and three continuous GPS stations.

GPS observations were processed with the GAMIT/GLOBK software suite (Herring *et al.* 2010a,b,c). GPS data from 25 International GNSS Service (IGS) stations were included to tie our local network to the ITRF2008 reference frame. We analysed the GPS data using a three-step approach (Reilinger *et al.* 2006). In the first step, we used GPS phase observations to estimate daily positions, together with atmospheric, orbital and Earth orientation parameters, using loose *a priori* constraints. In the second step we combined these positions and their covariances with global GPS solutions computed as part of MIT's processing for the IGS. We then examined the position time-series for outliers and offsets due to earthquakes or antenna changes and corrected these as appropriate. In a third step, we combined all of the data in a single solution, estimating positions and velocities for the period 1993–2014. In both the second and third steps we mapped the loosely constrained solution into a well-constrained reference frame by minimizing the position and velocity differences of selected sites with respect to *a priori* values defined by the IGS08 realization of the ITRF2008 reference frame (Altamimi *et al.* 2011). During this step, we used the 'stable-site' approach of Tregoning *et al.* (2013), by adopting their eight carefully selected reference sites with long-term stable behaviour that are less affected by earthquake deformations and hydrological loading.

Following the approach proposed by Reilinger *et al.* (2006), we accounted for temporally correlated errors by including a random-walk component estimated for each continuous site using the 'realistic sigma' algorithm of Herring *et al.* (2010c) (see also Reilinger *et al.* 2006). The median value of the random-walk, obtained from continuous time-series, is 0.3 mm/$\sqrt{\text{yr}}$. For campaign stations we have set a value of 1.0 mm/$\sqrt{\text{yr}}$ for the horizontal components. GPS time-series were inspected for instrumental changes as well as possible coseismic offsets from major earthquakes in the region. Since we did not have sufficient independent observational constraints on the coseismic displacement for the majority of the earthquakes that happened in the New Guinea region, we have opted to correct for coseismic offsets by inspecting GPS time-series themselves. We have corrected for the 1999 Mw 6.4 event, 20 km north of Lae, and the 2001 Mw 6.4 earthquakes near Bulolo (16 km north of Lae). The time-series of VANI and ANGS sites have been inspected for the effect of the 1998 Aitepe earthquake and a short post-seismic relaxation has been observed only in VANI. However, to avoid any post-seismic contamination of the linear rate, we opted to estimate the velocity using only the observations after 4 yr from the earthquake, extending between 2003 and 2008. As observations of sites northwest of Madang were obtained before and after the 2002 Mw 7.6 Wewak earthquake, we have modelled time-series using a linear combination of a secular interseismic rates and a logarithmic term with 10 d decay time, in order to take into account the post-seismic transient effect. We have chosen the decay constant that reduces the WRMS of the time-series residuals. We have excluded from our analysis the site BUTM, because it has been observed only twice after the Wewak earthquake, which resulted in an unconstrained fit of a logarithmic decay function. We have verified also the possible effect of the Solomon Sea 2007 Mw 8.1 earthquake for sites located in the Aure Fold-and-Thrust Belt region, using the surface displacements predicted by the model of Tregoning *et al.* (2013). However, the expected coseismic offset estimates were less that 1 mm, so we do not correct for this particular earthquake. We did not correct for Mw 6.7 Kutubu earthquake (New Guinea Highlands) because most of the stations that may have been influenced by this earthquake were first measured after the 2000 earthquake had occurred. Other sites that were measured before these events in the southern Highlands Fold-and-Thrust belt were too far away from this earthquake to be offset, and no jumps were detected in their time-series. The WRMS fit of our solution with respect to the IGS08 is 0.43 mm yr^{-1}, and 0.56 mm yr^{-1} for the north and east components respectively. The GPS velocities and their uncertainties are shown in Fig. 3 and given in Table S1 of the supplementary material in an Australian-fixed reference frame.

We have combined our velocity field with the velocities published by Wallace *et al.* (2004), after rotating their velocities from ITRF2000 to an Australia-fixed reference frame using 16 common sites between the two velocity solutions and located in the stable part of the Australian and Pacific plates. For our analysis, we use only horizontal velocities: we do not use the vertical estimates since they have large uncertainties with respect to the expected vertical motion in the region and there is a considerable likelihood of height errors having been introduced through the use of tripod-mounted antenna at the campaign GPS sites.

3.2 Velocity field

Fig. 3 shows the derived horizontal velocity field (with 95 per cent confidence ellipses) with respect to an Australian-fixed reference frame. The new velocity field shows many distinct patterns. It confirms the overall NE-SW convergence between the Australian and Pacific plates with a rate of ∼111 mm yr^{-1}. The striking features of the velocity field are: (i) the high convergence on the Ramu-Markham fault accommodating under-thrusting of the New Guinea Highlands beneath the Finisterre terrane, consistent with previous studies (Stevens *et al.* 1998; Tregoning *et al.* 1998; Wallace *et al.* 2004), (ii) the decrease of the relative velocity magnitude from ∼24 mm yr^{-1} south of the New Guinea Trench (at sites ANGS, VANI and BEWA) to ∼3 mm yr^{-1} in the southern Highlands Fold-and-Thrust Belt (sites TELE, TABU and TAB2). However, the lack of GPS spatial coverage makes this gradient poorly constrained east of 142°E, (iii) the tendency for rates to decrease from east to west across the Adelbert range (3.5–4°S; Fig. 3), delineating the eventual northeastern boundary of the New Guinea Highlands block that extends west of the Ramu-Markham fault.

Velocities south of the Finisterre Range and north of the Papuan Peninsula show different southwestward motion, distinct from the New Guinea Highlands block, with a likely anticlockwise rotation (Fig. S1). KAIN, BULO and KERE stations show a significant velocity of ∼9.0±1.4 mm yr^{-1} with respect to the Australian Plate, indicating that the boundary of the rigid Australian Plate lies south of those stations, likely along the Aure Fold-and-Thrust Belt (Fig. 3).

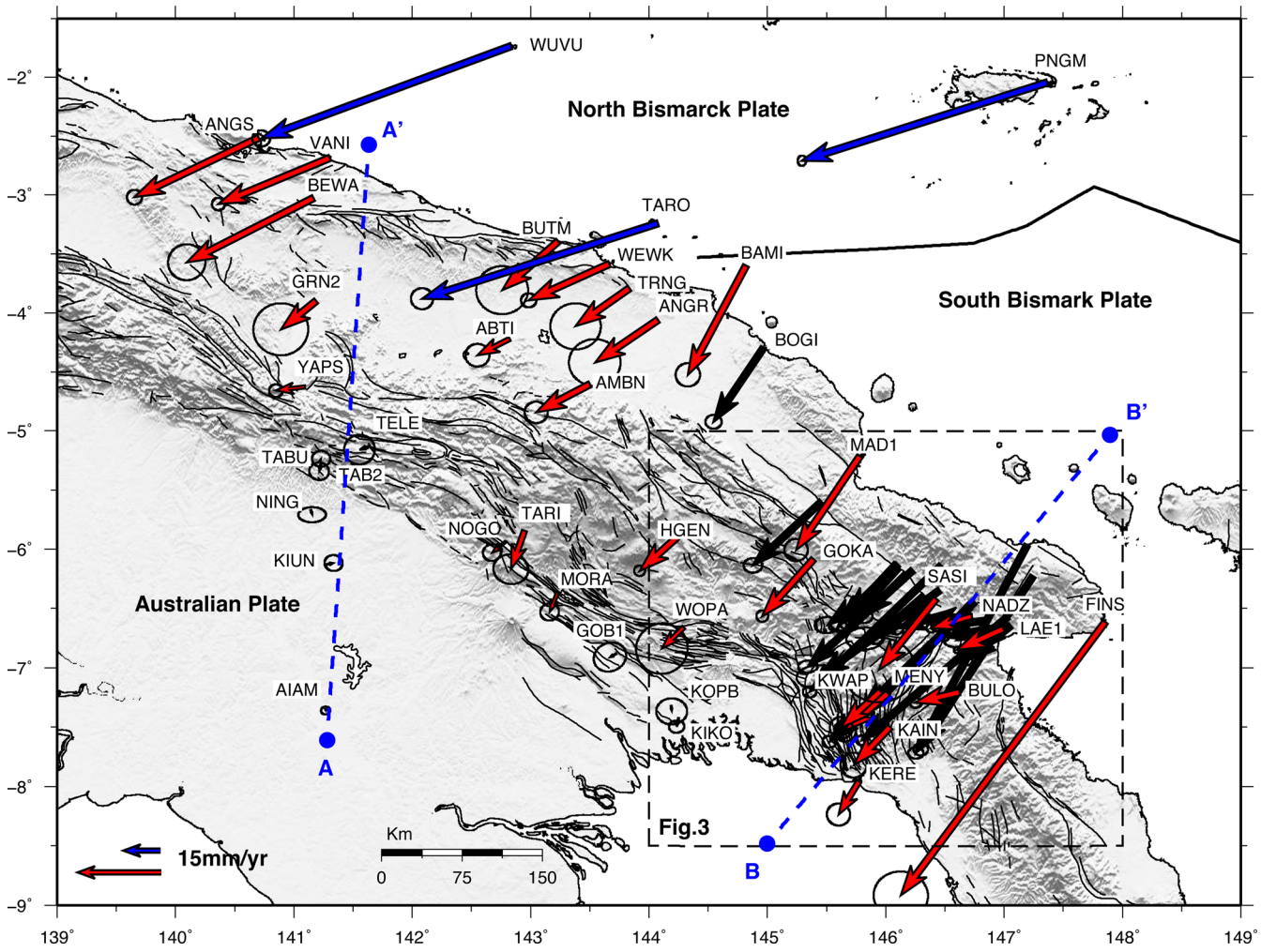

Figure 3. The GPS velocity field and 95 per cent confidence interval ellipses with respect to the Australian Plate. Red and blue vectors are the new calculated field and black vectors are from Wallace *et al.* (2004). The dashed rectangle shows the area of Fig. 3. The blue dashed lines correspond to the location of profiles shown in Fig. 4. Note that the velocity scales for the red and blue vectors are different (see the lower right corner for scales). The black velocities are plotted at the same scale as the red vectors.

In order to increase our understanding of the deformation mechanisms relative to these changes, as well as the spatial variation in crustal strain rates, we construct an elastic block model which we constrain with GPS velocities, geologic and seismological data.

4 KINEMATIC INTERPRETATION

4.1 Modelling approach

As described previously, the tectonics of PNG involves rapid crustal block rotations and high rates of strain accumulation in regions adjacent to active plate boundaries. Thus, the estimation of tectonic blocks rotations from interseismic GPS velocities needs to account for the elastic strain due to locking on block bounding faults. An elastic block model as described by (McCaffrey 2005; Meade & Hager 2005) is able to decompose the elastic deformation and the motion from block rotations in GPS velocities and therefore enables describing faults proprieties accommodating the deformation within the northwestern region of PNG.

We use the block model inverse approach in DEFNODE (McCaffrey 2005; McCaffrey *et al.* 2013), to invert velocities and earthquake slip vectors to solve simultaneously for the angular velocities of blocks and locking on block boundary faults. The optimization problem is solved using the simulated annealing method (Press *et al.* 1989) by minimizing the reduced chi-square of the misfit to the weighted data. DEFNODE adopts a backslip approach (Savage 1983) and the elastic half-space formulation of Okada (1985) to account for strain accumulation on block bounding faults, and the locking on faults is parameterized by the coupling coefficient ϕ, defined as the ratio between the short- and long-term slip rates. This parameter can be estimated in the inversion along with the angular block velocities.

Here we use our newly calculated velocity field, along with the published velocities of Wallace *et al.* (2004), to better constrain the motion in the southern part of the Ramu-Markham fault. We have discarded all the velocities that have been derived from only two observations. We also include the velocity estimates from Tregoning *et al.* (1999) to constrain the motion of the South Bismarck Plate, after aligning them to an Australian-fixed reference frame. Because this solution was calculated in ITRF97 reference frame, we have down-weighted the velocity uncertainties by a factor of two in order to account for errors that might be introduced from the discrepancies of reference frames. In addition to our regional GPS network, we have included 25 well-distributed continuous

stations on the Australian and Pacific plates in order to constrain the angular velocity of the large bounding plates. To the west of the Aure Fold-and-Thrust Belt, velocities from sites GOBE, TARI, MORA and IAGI show an inconsistent pattern of motion with the regional tectonic style, which we do not fully understand and we speculate that might be related to frequent landslides in this region. Therefore, we have excluded them from the inversion. In addition to GPS velocities described previously, we have used 241 earthquake slip vectors. Earthquake slip vectors azimuths were calculated from the global CMT focal mechanisms catalogue (Ekström *et al.* 2012) for shallow earthquakes with depths less than 40 km and we have assigned an uncertainty of 15° to all events (given the complexity of plate boundary in the PNG).

4.2 Blocks and fault geometries

The new GPS velocities presented in this study allow us to verify the nature of these tectonic boundaries and understand the mechanisms behind the long-term geologic deformation.

Here, we suggest a new model geometry based on seismicity, mapped faults (Baldwin *et al.* 2012; Davies 2012) and the GPS velocity field, revising the block model published by Wallace *et al.* (2004). We have augmented our blocks boundary definitions with the mapped fault lineations from the Coordinating Committee for Geoscience Programs in East and Southeast Asia (CCOP) 1:2000000 geological map of SE Asia (Fig. 1). We use eight blocks to describe the regional motion. We use the previously defined Woodlark Block, extending from the Woodlark seafloor-spreading centre to the New Britain Trench, and we do not take include the Trobriand microplate (Kington & Goodliffe 2008) since we do not have GPS data from this region. The motion of this block has been constrained using additional velocities from Wallace *et al.* (2014). The South Bismarck Plate extends as a backarc behind the New Britain Trench in the south to the transform fault zone along the BSSL. Tregoning (2002) showed that the relative motion of sites north of the BSSL (KAVI, WUVU and MANU) is systematically different from rigid Pacific Plate motion, favouring the hypothesis that the Manus Trench is an active plate boundary, albeit at a slow rate ($<$1 cm yr^{-1}). In the present study, we have included, in addition to the three campaign sites, a new campaign site (TARO) north of Wewak and the continuous GPS site (PNGM) on Manus Island, using time-series spanning over 6 yr. The estimated velocity of this site shows a residual with respect to the Pacific Plate, after accounting for transient post-seismic deformation associated with the 2002 Mw 7.6 Wewak earthquake, of 5 $\pm$ 0.6 and 3.5 $\pm$ 0.6 mm yr^{-1} for the northern and eastern components respectively, in agreement with the northward systematic pattern to the residuals shown by Tregoning (2002). Therefore we included in our model the North Bismarck microplate to the north of the BSSL and Manus Basin.

In our study, we have modelled the Papuan Peninsula as a separate block (PPBL) from the main New Guinea Highlands block, in contrast with previous studies (Wallace *et al.* 2004). In the southwest we define the boundary between the Australian and the Highlands blocks as the southernmost expression of the Highlands Fold-and-Thrust Belt. The northern boundary of the New Guinea Highlands block is defined as the Bewani-Torricelli fault zone, which links in the east to the offshore transform faults in the Bismarck Sea (BSSL), and to the Yapen fault in the west.

We have included in our model a separate Adelbert microplate (ADBL) northwest of the Finisterre Range (Fig. 1), bounded by the Adelbert Range to the west of Madang, and by the Gogol fault

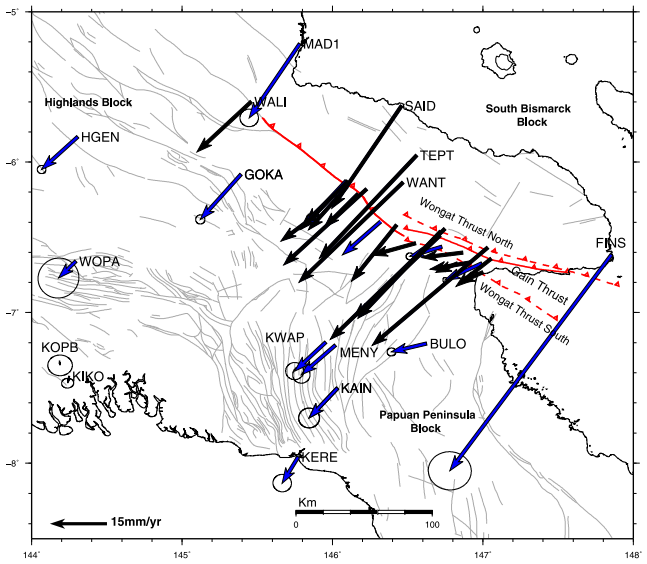

Figure 4. The GPS velocity field and 95 per cent confidence interval ellipses with respect to the Australian Plate zoomed on the dashed rectangle in Fig. 2 (blue vectors). The black vectors are from Wallace *et al.* (2004). For clarity purpose, we do not show uncertainties of black vectors. Faults lineaments are from the East and Southeast Asia (CCOP) 1:2000000 geological map. The red lines correspond to the Gain, Wongat Thrust South and North Traces, and the Ramu Markham fault from Abbott *et al.* (1994a).

on the southwest flank of the Adelbert Ranges (Fig. 1). Abbott (1995) and Wallace *et al.* (2004) previously speculated about the existence of this block based on geological observations and the northeast-southwest zone of seismicity extending north of Madang into the South Bismark Sea. Based on a plate reconstruction model, Holm & Richards (2013) suggested that the Adelbert microplate was formed following the fragmentation of the South Bismarck Plate in response to the collision with the thickened crust of the Bundi-Owen Stanley suture zone. Moreover, the topographic contrast between the Adelbert and Finisterre ranges may also be a result of the differential motion between the Adelbert microplate and the South Bismarck Plate.

Unlike previous active tectonics studies in PNG (Stevens *et al.* 1998; Wallace *et al.* 2004), we considered the surface expression of the southern part of the Ramu-Markham ramp and detachment fault to be north of Lae and the Ramu-Markham Valley, following the Gain Thrust (Fig. 4). This geometry is consistent with the Out-of-Sequence (OOS) Thrust model proposed by Abbott *et al.* (1994a), who showed that the Gain Thrust is a likely active structure, since it cuts the colluvium. The lack of seismicity in the upper 10 km in the Lae region due to the presence of 5 to 6 km weak layer of sediments (Kulig *et al.* 1993) may suggests that this region is deforming without elastic stain accumulation. On the other hand, our proposed geometry is inconsistent with inferred geological uplift in the region ($\sim$2 mm yr^{-1} in Lae city) (Crook 1989), and the projection of the Atzera Anticline (an actively growing anticline) to the south of Lae, as well as the inferred projection of the RMFZ beneath Lae based on seismological studies (e.g. Kulig *et al.* 1993). If much of the relative plate motion is currently being accommodated by the Gain thrust, this is also consistent with the hypothesis of Abbott *et al.* (1994a) that the Wongat Thrust south Trace ceased activity during the last $\sim$100 Ka, that the Gain Thrust was initiated and is still active to the present-day. An alternative model, which also produces a good fit to the data (Wallace *et al.* 2004), assumes that the

Ramu-Markham fault projecting south of Lae is the major boundary separating the upper plate of South Bismarck Block and the New Guinea Highlands, which is more consistent with seismological and geomorphological evidence (Crook 1989; Kulig *et al.* 1993). To fit the GPS data with this scenario, Wallace *et al.* (2004) assumed the Ramu-Markham fault is a shallowly dipping detachment at depth (>20 km), and steepens to a ramp from ∼20 km depth to within 1 km of the surface beneath Lae, and then shallows again to a low angle detachment projecting beneath Lae. Full locking of the ramp and shallow detachment structure provides a reasonable fit to the data in the Lae area as well. Locking of the shallow detachment leads to a surface deformation pattern that mimics the lower plate.

The profile B–B′ in Fig. 6 shows a comparison between the two alternative models, showing the location of the velocity magnitude change in the SW–NE direction across the foothills line of the Finisterre mountains. Although the fit to the GPS velocities is reasonably similar in both scenarios, the GPS observations are fit best when we use the Gain Thrust as the primary boundary, rather than the projection of the Ramu-Markham fault south of Lae($\chi^2/\mathrm{dof} = 1.7$ versus $\chi^2/\mathrm{dof} = 2.7$ for alternate model). It is also possible that both structures (Gain Thrust and Ramu-Markham fault) are accommodating active deformation, but we do not have sufficient GPS data to reliably test this hypothesis. Based on the better fit to the Gain Thrust scenario, we prefer the hypothesis that the Gain Thrust is currently accommodating a larger proportion of the plate motion. However, given the geological and seismological evidence that the Ramu-Markham fault projects to the south of Lae, the higher rates observed for the Gain Thrust may only be temporary.

As part of the inversion, we solved for the degree of coupling along the Ramu-Markham fault, the New Guinea Trench, the western BSSL, the New Guinea Highlands thrust and the Adelbert fault. The rest of the fault segments, where we do not have good GPS coverage, have been either defined as locked to a depth of 15 km or as freely slipping boundaries. To first order, we have chosen a simplistic geometry of the modelled fault in order to not over fit the GPS velocities and to reduce the number of estimated parameters. We estimated the coupling along the Ramu-Markham fault at each node (in contrast to the New Guinea Trench inversions), because here we have good spatial coverage of GPS sites; hence, a greater likelihood of being able to recover an accurate, spatially varying slip deficit estimate. To regularize the solution of the coupling along the Ramu-Markham fault/Gain Thrust, we applied smoothing constraints on the gradient of the along-strike coupling coefficient. The best smoothing coefficient was chosen assuming a trade-off between the minimum χ^2/dof statistics and reasonable distribution of the coupling along the fault plane.

We assume the New Guinea Trench is the boundary between the Pacific/North Bismarck plates and the New Guinea mainland. The interface is modelled as a 25° dipping surface beneath the PNG mainland (Tregoning & Gorbatov 2004). Seismicity clusters are concentrated mainly east of 141°E along this trench and indicate that active deformation extends south to 3°S (Fig. 1). As the GPS sites distribution along this trench does not allow for a resolution of the coupling in the downdip direction, we have adopted a simple parameterization of the coupling distribution as two uniform parts along-strike. Then we have run a series of experiments, varying the coupling ratio from 0 to 100 per cent. Our results suggested that the best fit is reached with a coupling of 20 and 10 per cent in the western and eastern segments, respectively. The relatively low coupling observed on the New Guinea Trench coincides with moderate seismicity along the lowest coupling area between 139°E and 135°E (Okal 1999). The result of low coupling suggests that the New Guinea Trench is mostly creeping, perhaps with some small asperities surrounded by creeping areas, which is compatible with the frequent, moderate seismicity observed at the New Guinea Trench.

4.3 Model results

The advantage of using a block model to represent the present-day crustal motion arises from its flexibility to allow us to test different plate boundary geometries and check which changes provide significant improvements in fitting the observations and thus in our understanding of the kinematics of the studied region (Payne *et al.* 2012). In order to check the significance of our proposed geometry, we have first constructed a block model assuming a single New Guinea Highlands block as suggested by Wallace *et al.* (2004). This model produces a $\chi^2/\mathrm{dof} = 3.43$ and does not provide a good fit to the velocities south of Finisterre terrain and Aure Fold-and-Thrust Belt (KWAP, MENY, KAIN, KERR, LAE1, NADZ). As we separate the New Guinea Highlands block into a Papuan Peninsula block (PPBL) and a New Guinea Highlands block (HLBL), without considering a forearc block (FORE) in the north (just to the south of the New Guinea Trench), we observe a decrease of the χ^2/dof to 2.56. The two sites located in the Adelbert Range (BOGI and BAMI) show a distinct motion and their velocities do not fit either the south Bismarck block or the New Guinea Highlands block. A model without an independent Adelbert block (but with a free PPBL, HLBL, and FORE blocks) produces a slightly higher $\chi^2/\mathrm{dof} = 2.29$, suggesting that the Adelbert block is a separate entity. Finally, including a FORE block gives a much improved fit with $\chi^2/\mathrm{dof} = 1.75$. To determine if the improvement in fit of the model resulting from the addition of these new blocks is statistically significant, we have used the F-ratio test with a confidence level of 95 per cent between the two models (Stein & Gordon 1984). We found that the improvement in fit after splitting the New Guinea Highlands block is significant and greater than expected by chance (Table S3 for F-test summary). Finally, for the validation of our preferred geometry of the southern boundary of the South Bismarck Plate, we compare our preferred model (where the Gain Thrust currently takes most of the plate motion), with the geometry of Wallace *et al.* (2004), where the Ramu Markham fault projects to the south of Lae. The latter model produces a χ^2/dof value of 2.77, thus the improvement in fit from our preferred model is statistically significant.

Fig. 5 shows the comparison between the observed and the calculated velocities for our preferred model. The χ^2/dof misfit of our preferred model is 1.75 for 505 observations (132 GPS velocities and 241 earthquake slip vectors) and 57 estimated parameters. The residual GPS velocities for the most of our study area are within their uncertainties and do not show systematic patterns (Figs 2S and 3S), with the exception of the segment south of Wewak, which we think is due to residual post-seismic signal from 2002 Wewak earthquake. The normalized rms for the GPS residuals is 1.39 mm yr^{-1} (1.32 mm yr^{-1} for the east component and 1.45 mm yr^{-1} for the north component) and the weighted rms are 0.49 and 0.55 mm yr^{-1} for the eastern and northern components, respectively.

Fig. 6 shows the observed and predicted velocity profiles normal and parallel to the main structures. In general GPS velocities agree with the model, within their uncertainties, for both AA′ and BB′ profiles. The profile AA′ shows that the model reproduces the step observed in the GPS velocities across the two main boundaries: south of the Highlands Fold-and-Thrust Belt and the Bewani-Torricelli fault. The profile BB′ fits the observed velocities well except at the

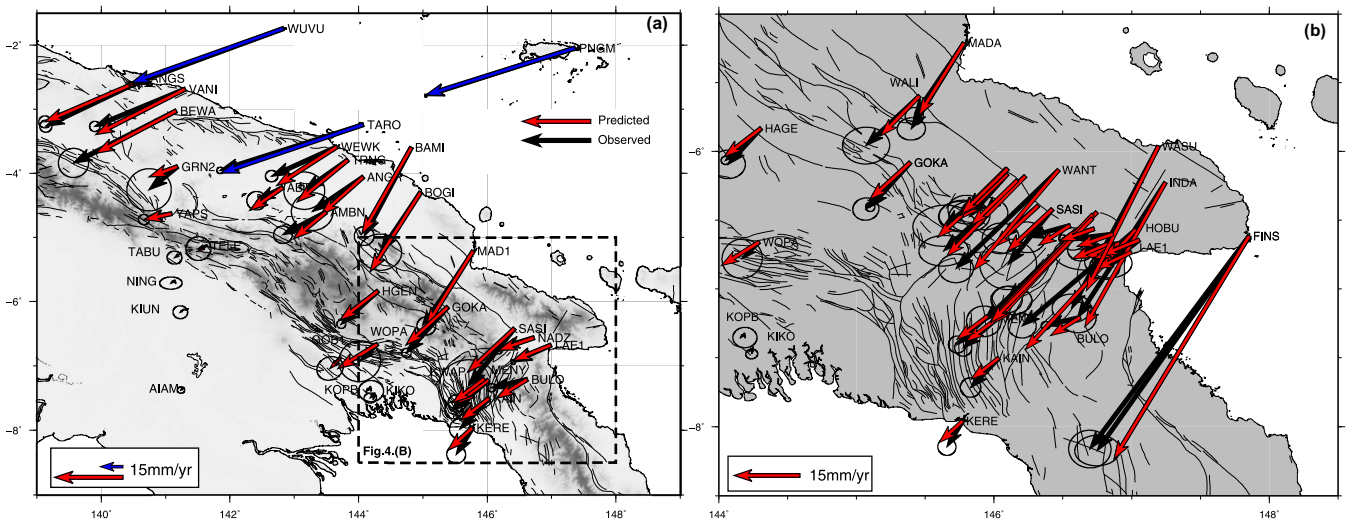

Figure 5. Observed (red) and modelled (black) GPS velocities (see the text for discussion). The dashed blue box in (a) shows the region of Fig. 4(b). Error ellipses are 95 per cent confidence interval. Note that for subfigure (a), the velocity scales for the red and blue vectors are different (see the lower right corner for scales).

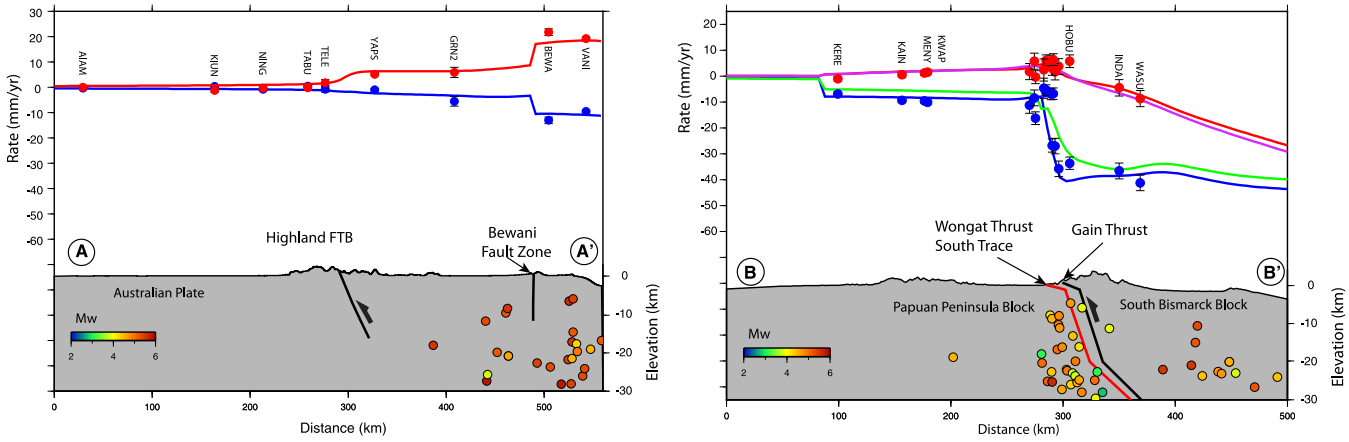

Figure 6. Profiles A–A′ and B–B′ from Fig. 2 showing model fit to GPS observations. Red symbols and lines are the GPS observed and modelled velocities, respectively, for the profile-normal component. Blue symbols and lines correspond to the profile-parallel component. The green and pink lines corresponds to the model using the Ramu-Markham fault geometry from Wallace *et al.* (2004), south of Lae. Grey profiles show the projected topography. The seismicity is from the ISC catalogue for events > Mw3.5 (1960–2011).

far northeastern end of the profile where the downdip extent and geometry of the Ramu-Markham fault is largely unconstrained.

5 DISCUSSION

5.1 Slip partitioning in New Guinea

Previous studies showed some evidence of the existence of an active subduction zone where the Pacific Plate underthrusts northern PNG, known as the New Guinea Trench. Hamilton (1979) showed seismic reflection profiles along the Wewak segment indicating south-dipping underthrusting. Using a more accurate data set of *P*- and *S*-wave arrival times and hypocentre locations, Tregoning & Gorbatov (2004) supported these observations by showing a south-west dipping slab in the eastern part of the New Guinea Trench. The relative motion across this boundary has been the subject of speculation and has never been quantified. Kroenke (1984) and Cloos *et al.* (2005) suggested that New Guinea Trench is a relict of an earlier subduction and that only the Wewak eastern segment has been reactivated. Conversely, our model predicts oblique convergent motion across the trench up to ∼66.4 ± 1.6 mm yr^{-1} taken up by the subduction of the Pacific Plate at the New Guinea Trench, including the western segment between 140°E and 142°E, where a coherent pattern of crustal deformation from GPS is available. Given the total relative motion of 111 mm yr^{-1} between the Pacific and Australian plates, the New Guinea Trench accounts for ∼59 per cent for the margin normal (convergent) component and 66 per cent for margin parallel (left-lateral strike-slip) motion, while ∼12 per cent of both of shortening as well as shear are distributed between the Bewani-Torricelli fault and the west New Guinea Highlands fault.

It has been recognized that an active fault zone (the Bewani-Torricelli fault zone) runs through the narrow band of eroded mountains known as the Bewani and Toricelli mountains. Dow (1977) interpreted the intensively faulted Pliocene sediments north of the Bewani-Torricelli mountains as an indication of recent activity of this fault zone. However, the rate and kinematics of activity along this boundary has never been quantified. Sapiie & Cloos (2004) suggested that this fault system is the major boundary which

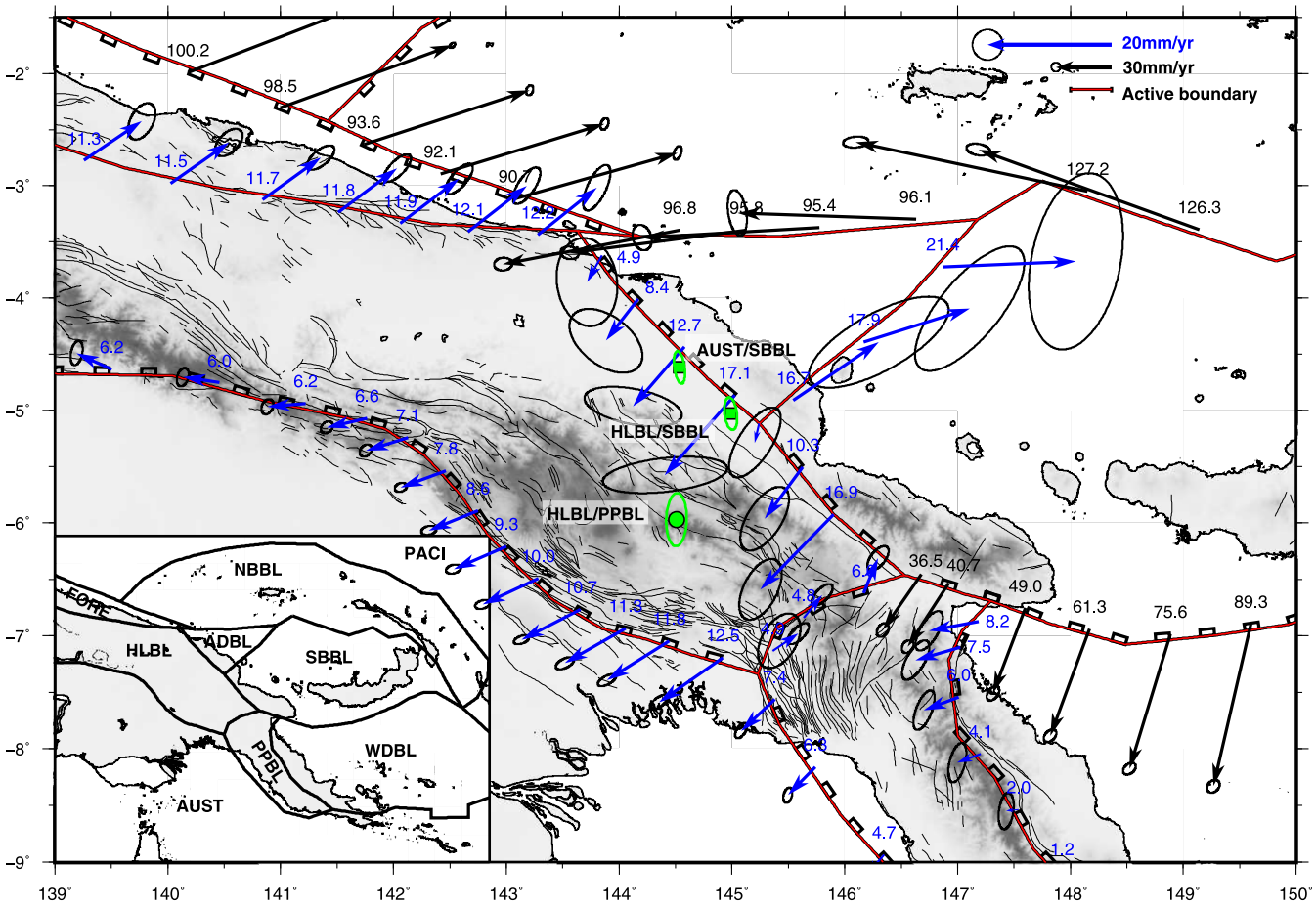

Figure 7. Predicted relative motion (indicated by arrows) across block boundaries based on our kinematic model and corresponding error ellipses (grey). Green dots indicate the location of the best-fit Euler poles with their error ellipses. Euler vectors are for the second plate relative to the first. Block-bounding faults are shown as red/black lines with small rectangles on the hanging wall sides. AUST, Australia; PACI, Pacific; HLBL, Highlands block; SBBL, South Bismarck block; PPBL, Papuan Peninsula block; WDBL, Woodlark block; ADBL, Adelbert block. Note that the velocity scales for the red and blue vectors are different (see the lower right corner for scales).

accommodates most of the motion between the Australian and Pacific plates. However, our GPS observations in the region clearly show that strain is partitioned between the Bewani/Torricelli ranges and the New Guinea Trench. Our model predicts a sinistral strike-slip motion of 6.8 to 8.9 ± 0.5 mm yr^{-1} with an azimuth of ∼270° along the fault lineation, which represents ∼6 per cent of margin-parallel component of Australia/Pacific relative plate motion. The New Guinea Highlands belt accommodates some of the oblique convergence between the Pacific and Australian plates and the estimated amount of relative motion across this boundary has varied in different studies. Abers & McCaffrey (1994) suggested a rate between 4 and 9 mm yr^{-1} of convergence, while Wallace *et al.* (2004) estimated this rate to be ∼14 mm yr^{-1} near 142 E decreasing to ∼2 mm yr^{-1} near 145 E. Our transect of sites along the western PNG border provides the most comprehensive observation to date of the deformation rate in the western New Guinea Highlands, allowing us to better constrain the deformation rates on the boundaries of the New Guinea Highlands block, and the block kinematics. The much improved GPS coverage in the Highlands show that rather than rotating anticlockwise as suggested by Wallace *et al.* (2004; determined from a sparser data set largely focused in the eastern Highlands), that the New Guinea Highlands block is actually rotating clockwise about a pole to the northwest of the New Guinea Highlands. This produces a westward decrease in deformation rate in the fold and thrust belt in contrast to the westward increase required by Wallace *et al.* (2004) anticlockwise rotation about a pole to the southeast. Our model predicts an average of ∼11 mm yr^{-1} of convergence in the eastern part of the New Guinea Highlands belt, with a decrease of the relative motion towards the west from 12 ± 0.7 to 6.8 ± 0.7 mm yr^{-1} (Fig. 7). West of 142°E, our model predicts a transition to a dominant left-lateral strike-slip system with slip rates of 6–7 mm yr^{-1}. This is compatible with observed seismicity and focal mechanisms of the area, as suggested by Abers & McCaffrey (1988) who showed the existence of strike-slip with left-lateral motion earthquake mechanisms between 4.1°S and 4.3°S (between 139°E and 140°E). The new kinematic scenario we present here helps to reconcile the transition from thrusting to left-lateral strike-slip in West Papua, and helps to conceptually link the tectonics of the New Guinea Highlands with those in West Papua (Indonesia).

The concentration of the seismic activity in the fold and thrust belt of the New Guinea Highlands block, has led previous studies to assume that the majority of deformation in the New Guinea Highlands is restricted to the fold and thrust belt (Wallace *et al.* 2004). However, recent geologic investigations showed a series of NE–SW transfer faults in the central and east New Guinea Highlands (White *et al.* 2013), which could accommodate deformation within the thrust-faulted New Guinea Highlands. To test for the role

of permanent internal block strain rate, we solved for an additional parameter corresponding to the three components of the horizontal strain rate tensor within the New Guinea Highlands block, to uniformly strain the block. However, this did not lead to any improvement in the χ^2/dof statistics (χ^2/dof = 1.9), suggesting that the block, as defined in our study, is likely behaving as a largely rigid body.

5.2 Implications for the BSSL

As mentioned in Section 4.2, we have defined the North Bismarck microplate as the block between the Manus Trench and the BSSL (Taylor *et al.* 1991; Tregoning *et al.* 1999). The subduction process in the Manus trench is often thought to have terminated and there is no strong seismic or geologic available evidence of ongoing under-thrusting beneath the North Bismarck Plate. The earlier GPS investigations of Tregoning *et al.* (1998) did not find conclusive evidence for a North Bismarck Plate. However, with more observations, Tregoning (2002) showed that the relative motion of the sites located north of the BSSL is significantly different from the Pacific Plate. Our model predicts 3 to 5 $\pm$1.4 mm yr^{-1} convergence along the Manus Trench, consistent with previous geodetic studies (Tregoning 2002; Wallace *et al.* 2004). On the southern side of the North Bismarck Plate, the left-lateral fault zone BSSL takes most of the relative motion between the Pacific and the south Bismarck plate. We predict a relative motion in the western boundary of the BSSL fault segment, east of the triple junction, with a strike-slip component of $\sim$95 $\pm$ 2.0 mm yr^{-1}, and a convergent component of $\sim$15 $\pm$ 1.9 mm yr^{-1} in the most western part of the lineation. Our estimate is consistent with the predominantly shallow left-lateral focal mechanisms that have occurred in this region (Fig. 7).

The shift from mostly strike-slip and extension on the BSSL to the east compared with a compressional component to the west was also observed in the block model of Wallace *et al.* (2004), and is related to the orientation of the BSSL there combined with anticlockwise rotation of the North Bismarck Block with respect the South Bismarck Plate, leading to strain partitioning into multiple fractures accommodating the oblique convergence across the western portion of the BSSL (Llanes *et al.* 2009).

5.3 The kinematics of the Finisterre and Adelbert collision

We set the western boundary of the ADBL to follow the topographic contrast along the Adelbert Range, northwest of Madang (Fig. 1), while taking into account the lateral variation of the observed velocity field further north (Fig. 3). The difference in motion between BAMI and BOGI in the east and most of the site velocities west of the proposed boundary indicate that the western ADBL boundary is taking up the relative motion between the Adelbert and the New Guinea Highlands blocks. Our model shows a small convergence between 5 and 16 mm yr^{-1}, decreasing towards the north. The eastern boundary of the ADBL accommodates the relative motion between the Adelbert and the South Bismarck Block with a rate of 16 and 21 mm yr^{-1} of left lateral motion increasing towards the north. This result is still uncertain given that the ADBL motion is defined by only two site velocities, while the slip-vectors constraints provide information only for the offshore segment of the Adelbert fault (Fig. 7).

Further south, our modelling results support a significant increase in the motion along the Ramu-Markham fault from 10 mm yr^{-1} to 40 mm yr^{-1} south of the Huon Peninsula and reaching $\sim$45 $\pm$ 1.7 mm yr^{-1} in the junction with the New Britain Trench, and increasing to 132 mm yr^{-1} at 152E along the New Britain Trench. Our estimates are consistent with those suggested by Tregoning *et al.* (1998) and Wallace *et al.* (2004).

5.4 The Papuan Peninsula Block

We modelled the Owen Stanley fault as the boundary between the Woodlark Basin and the Papuan Peninsula, following the southwest boundary of the Papuan ultramafic belt (Owen-Stanley metamorphics) in line with Fitz & Man (2013 and Davies *et al.* (1987). We predict a convergence between $\sim$2 and 7 mm yr^{-1} increasing to the northern termination at the junction with the Ramu-Markham fault. This is slightly slower than the rate estimated by Wallace *et al.* (2004), due to the fact that we partition the deformation between the Woodlark Plate and the New Guinea Highlands onto two structures (the Owen Stanley FZ, and the Aure Fold-and-Thrust Belt), rather than a single structure. The rates we obtain for the Owen Stanley fault are similar to those estimated by Wallace *et al.* (2014), using an extensive data set focused on SE PNG.

To the southwest, the boundary of the Papuan Peninsula with the Australian Plate corresponds with the Moresby Trough, accommodating a convergence on the order of 5 to 7 mm yr^{-1}. The southwestward significant motion observed at KERE, MORE and KAIN supports the idea that significant contraction occurs on the Moresby Trough, and this provides the first quantitative evidence for active convergence on this boundary. More GPS stations are needed south of the Aure Fold-and-Thrust Belt in the Papuan Peninsula in order to better constrain this motion.

The Aure Fold-and-Thrust Belt complex shows a distinct morphological structure composed of a combination of arc-shaped and roughly north-south striking folds and faults. The structure has been interpreted as the result of the westward movement of the Papuan Peninsula (Dow 1977; Wallace *et al.* 2004; Davies 2012). In our best-fit model the Papuan Peninsula (PPBL) is a separate block from the New Guinea Highlands and the PPBL limit corresponds to the E-W trending fault from the junction of the Ramu-Markham to the western Aure Fold-and-Thrust Belt. Despite the lack of shallow seismicity in this region delineating the trend of surface faulting, there are many mapped faults aligning with the Aure escarpment (Jenkins 1974). Our model predicts a counter-clockwise rotation of the PPBL, with a pole with respect to the New Guinea Highlands Block located at 144.55°E, 5.96°S. We predict a left-lateral motion with a 110° azimuth and a slip rate between 3.9 and 5 mm yr^{-1} along the boundary between the New Guinea Highlands Block and the Aure Tectonic belt. The location of the Euler pole and the observed gradual convergent motion, from GPS velocities (Fig. 3), in the E–W direction from the termination of the Owen Stanley fault to the Aure Trough, is consistent with the geomorphological pattern of easterly dipping folding structures.

Although we obtain an excellent fit to the GPS data assuming most of the deformation is produce by interaction of crustal blocks, is possible that the pattern of the surface deformation illustrated in the GPS velocity in eastern PNG might be influenced by deeper crust, mantle, and slab processes. More specific detailed seismological imaging studies and geodynamic modelling are needed to evaluate this.

6 CONCLUSION

We use our new GPS velocity field for the central and western PNG region and have used it to estimate the present-day active

deformation, updating previous studies (Tregoning *et al.* 1998; Wallace *et al.* 2004) and we present new kinematic constraints. Our kinematic modelling yields highly oblique convergence of ∼93 mm yr^{-1} across the New Guinea Trench, confirming that the New Guinea Trench is the principal active interplate boundary. We obtain a coupling coefficient for the New Guinea Trench of 10–20 per cent, suggesting that a large proportion of the plate motion is accommodated by aseismic creep. We show also that there is some partitioning of convergence between the New Guinea Trench, the Bewani-Torricelli fault zone and the southern Highlands Fold-and-Thrust Belt. The latter accommodates convergence between 6 and 13 mm yr^{-1}, decreasing in the West New Guinea Highlands towards a strike-slip regime, consistent with previous studies (Abers & McCaffrey 1988). We suggest that the New Guinea Highlands Block undergoes a clockwise rotation with respect to the Australian Plate in contrast to Wallace *et al.* (2004) who suggested anticlockwise rotation. The New Guinea Highlands block is a separate entity from the Papuan Peninsula and we predict that the boundary between the Highlands and Papuan Peninsula blocks accommodates 3–5 mm yr^{-1} left-lateral motion with normal fault convergence of ∼2.5 mm yr^{-1}. We show that Gain thrust is the current active boundary between the South Bismarck Plate and the New Guinea Highlands/Papuan Peninsula and we confirm the high strain gradient across the Ramu-Markham Valley associated with the Finisterre arc-continent collision, which results in a convergence of up to ∼40 mm yr^{-1}. Our kinematic model shows an active convergence along the Moresby Trough up to ∼7 mm yr^{-1}, revealing a potential tsunamogenic source in the region, which needs to be considered in future seismic hazard assessment.

ACKNOWLEDGEMENTS

We are grateful to the individuals who participated in GPS surveys over the past 20 yr in Papua New Guinea. We thank Geoffrey Abers and anonymous reviewer for their helpful reviews. This work was supported partially by ARC Linkage project LP110100525. We thank R. McCaffrey for providing DEFNODE.

REFERENCES

Abbott, L.D., 1995. Neogene tectonic reconstruction of the Adelbert-Finisterre-New Britain collision, northern Papua New Guinea, *Journal of Southeast Asian Earth Sciences,* **11,** 33–51.

Abbott, L.D., Silver, E.A. & Galewsky, J., 1994a. Structural evolution of a modern arc-continent collision in Papua New Guinea, *Tectonics,* **13,** 1007–1034.

Abbott, L.D., Silver, E.A., Thompson, P.R., Filewicz, M.V., Schneider, C. & Abdoerrias, 1994b. Stratigraphic constraints on the development and timing of arc-continent collision in northern Papua New Guinea, *J. Sediment, Res., Sect. B,* **64,** 169–183.

Abers, G. & McCaffrey, R., 1988. Active deformation in the New Guinea fold-and-thrust belt: Seismological evidence for strike-slip faulting and basement-involved thrusting, *J. geophys. Res.,* **93**(B11), 13 332–13 354.

Abers, G.A. & McCaffrey, R., 1994. Active arc-continent collision: Earthquakes, gravity anomalies, and fault kinematics in the Huon-Finisterre Collision zone, Papua New Guinea, *Tectonics* **13**(2), 227–245.

Altamimi, Z., Collilieux, X. & Métivier, L., 2011. ITRF2008: an improved solution of the International Terrestrial Reference Frame, *J. Geod.,* **85,** 457–473.

Baldwin, S.L., Fitzgerald, P.G. & Webb, L.E., 2012. Tectonics of the New Guinea region, *Annu. Rev. Earth Planet. Sci.,* **40,** 495–520.

Bird, P., 2003. An updated digital model of plate boundaries, *Geochem. Geophys. Geosyst.,* **4**(3), 1027, doi:10.1029/2001GC000252.

Borrero, J.C., Bu, J., Saiang, C., Uslu, B., Freckman, J., Gomer, B., Okal, E.A. & Synolakis, C.E., 2003. Field survey and preliminary modeling of the Wewak, Papua New Guinea earthquake and tsunami of September 9, 2002, *Seismol. Res. Lett.,* **74,** 393–405.

Cloos, M., Sapiie, B., van Ufford, A.Q., Weiland, R.J., Warren, P.Q. & McMahon, T.P., 2005. Collisional delamination in New Guinea: the geotectonics of subducting slab breakoff, in *Geological Society of America Special Papers,* Vol. 400, pp. 1–51, Geological Society of America, doi:10.1130/2005.2400.

Crook, K.A.W., 1989. Quaternary uplift rates at a plate boundary, Lae urban area, Papua New Guinea, *Tectonophysics,* **163,** 105–118.

Davies, H.L., 2012. The geology of New Guinea: the cordilleran margin of the Australian continent, *Episodes,* **35,** 87–102.

Davies, H.L. & the Wewak Survey Team, 2002. Preliminary results of the field survey, 2002 PNG earthquake at Wewak, *EOS, Trans. Am. geophys. Un.,* **83,** 47.

Davies, H.L., Lock, J., Tiffin, D.L., Honza, E., Okuda, Y., Murakami, F. & Kisimoto, K., 1987. Convergent tectonics in the Huon Peninsula region, Papua New Guinea, *Geo Mar. Lett.,* **7,** 143–152.

DeMets, C., Gordon, R.G., Argus, D.F. & Stein, S., 1994. Events of recent revisions to the geomagnetic reversal time scale on estimates of current plate motions, *Geophys. Res. Lett.,* **21,** 2191–2194.

Dow, D.B., 1977. *A Geological Synthesis of Papua New Guinea,* Bulletin 201, Bureau of Mineral Resources, Geology and Geophysics.

Ekström, G., Nettles, M. & Dziewonski, A.M., 2012. The global CMT project 2004–2010: centroid-moment tensors for 13,017 earthquakes, *Phys. Earth planet. Inter.,* **200–201,** 1–9.

Fitz, G. & Mann, P., 2013. Tectonic uplift mechanism of the Goodenough and Fergusson Island gneiss domes, eastern Papua New Guinea: constraints from seismic reflection and well data, *Geochem. Geophys. Geosyst.,* **14,** 3969–3995.

Hamilton, W., 1979. *Tectonics of the Indonesian Region,* US Gov. Print. Off., 345 pp.

Herring, T.A., King, R.W. & McClusky, S.C., 2010a. Introduction to GAMIT/GLOBK, Release 10.4, Dept. of Earth Atmos. and Planet. Sci., Mass. Instit. of Technol., Cambridge, MA, 48 pp.

Herring, T.A., King, R.W. & McClusky, S.C., 2010b. GAMIT Reference Manual, GPS analysis at MIT, Release 10.4, Dept. of Earth Atmos. and Planet. Sci., Mass. Inst. of Technol., Cambridge, MA, 171 pp.

Herring, T.A., King, R.W. & McClusky, S.C., 2010c. GLOBK: Global Kalman filter VLBI and GPS analysis program, Release 10.4, Dept. of Earth Atmos. and Planet. Sci., Mass. Inst. of Technol., Cambridge, MA, 91 pp.

Hill, K.C. & Hall, R., 2003. Mesozoic-Cenozoic evolution of Australias New Guinea margin in a west Pacific context, *Geol. Soc. Am. Spec. Pap.,* **372,** 265–290.

Holm, R.J. & Richards, S.W., 2013. A re-evaluation of arc-continent collision and along-arc variation in the Bismarck Sea region, Papua New Guinea, *Australian Journal of Earth Sciences,* **60**(5), 605–619.

Jenkins, D.A.L., 1974. Detachment tectonics in western Papua New Guinea, *Bull. geol. Soc. Am.,* **85**(4), 533–548.

Johnson, T. & Molnar, P., 1972. Focal mechanisms and plate tectonics of the southwest Pacific, *J. geophys. Res.,* **77,** 5000–5032.

Kington, J.D. & Goodliffe, A.M., 2008. Plate motions and continental extension at the rifting to spreading transition in Woodlark Basin, Papua New Guinea: can oceanic plate kinematics be extended into continental rifts? *Tectonophysics,* **458,** 82–95.

Kroenke, L.W., 1984. Cenozoic tectonic development of the southwest Pacific, *UN Econ. Soc. Comm. Asia Pacific Tech. Bull.,* **6,** 1–126.

Kulig, C., McCaffrey, R., Abers, G.A. & Letz, H., 1993. Shallow seismicity of arc-continent collision near Lae, Papua New Guinea, *Tectonophysics,* **27,** 81–93.

Llanes, P., Silver, E., Day, S. & Hoffman, G., 2009. Interactions between a transform fault and arc volcanism in the Bismarck Sea, Papua New Guinea, *Geochem. Geophys. Geosyst.,* **10,** Q06013, doi:10.1029/2009GC002430.

McCaffrey, R., 1992. Oblique plate convergence, slip vectors, and forearc deformation, *J. geophys. Res.,* **97,** 11 953–11 966.

McCaffrey, R., 1996. Slip partitioning at convergent plate boundaries of SE Asia, in Tectonic Evolution of SE Asia Symposium, *Geol. Soc. Special Publication,* **106,** 3–18.

McCaffrey, R., 2005. Block kinematics of the Pacific-North America plate boundary in the southwestern United States from inversion of GPS, seismological, and geologic data, *J. geophys. Res.,* **110,** B07401, doi:10.1029/2004JB003307.

McCaffrey, R., King, R.W., Payne, S.J. & Lancaster, M., 2013. Active Tectonics of Northwestern US inferred from GPS-derived Surface Velocities, *J. geophys. Res.,* **118,** 709–723.

McClusky, S., Mobbs, K., Stoltz, A., Barsby, D., Loratung, W., Lambeck, K. & Morgan, P., 1994. The Papua New Guinea satellite crustal motion surveys, *Aust. Surv.,* **39,** 194–214.

Meade, B.J. & Hager, B.H., 2005. Block models of crustal motion in southern California constrained by GPS measurements, *J. geophys. Res.,* **110,** B03403, doi:10.1029/2004JB003209.

Okada, Y., 1985. Surface deformation due to shear and tensile faults in a half-space, *Bull. seism. Soc. Am.,* **75,** 1135–1154.

Okal, E.A., 1999. Historical seismicity and seismotectonic context of the Great 1979 Yapen and 1996 Biak, Irian Jaya earthquakes, *Pure appl. Geophys.,* **154,** 633–675.

Payne, S.J., McCaffrey, R., King, R.W. & Kattenhorn, S.A., 2012. A new interpretation of deformation rates in the Snake River Plain and adja- cent Basin and Range regions based on GPS measurements, *Geophys. J. Int.,* **189,** 101–122.

Pegler, G., Das, S. & Woodhouse, J.H., 1995. A seismological study of the eastern New Guinea and western Solomon Sea regions and its tectonic implications, *Geophys. J. Int.,* **122,** 961–981.

Press, W.H., Flannery, B.P., Teukolsky, S.A. & Vetterling, W.T., 1989. *Numerical Recipes,* Cambridge Univ. Press.

Reilinger, R. *et al.*, 2006. GPS constraints on continental deformation in the Africa-Arabia-Eurasia continental collision zone and implications for the dynamics of plate interactions, *J. geophys. Res.,* **111,** B05411, doi:10.1029/2005JB004051.

Sapiie, B. & Cloos, M., 2004. Strike-slip faulting in the core of the Central Range of west New Guinea: Ertsberg Mining District, Indonesia, *Bull. geol. Soc. Am.,* **116**(3–4), 277–293.

Savage, J.C., 1983. A dislocation model of strain accumulation and release at a subduction zone, *J. geophys. Res.,* **88,** 4984–4996.

Stein, S. & Gordon, R.G., 1984. Statistical tests of additional plate boundaries from plate motion inversions, *Earth planet. Sci. Lett.,* **69,** 401–412.

Stevens, C., McCaffrey, R., Silver, E.A., Sombo, Z., English, P. & van der Kevie, J., 1998. Mid-crustal detachment and ramp faulting in the Markham Valley, Papua New Guinea, *Geology,* **26,** 847–850.

Taylor, B., Crook, K., Sinton, J. & Petersen, L., 1991. Manus Basin, Papua New Guinea, SeaMARC II sidescan sonar imagery and bathymetry, scale 1:250,000, *Pacific Seafloor Atlas,* sheets 1–6, Hawaii Institute of Geophysics, Honolulu.

Tregoning, P., 2002. Plate kinematics in the western Pacific derived from geodetic observations, *J. geophys. Res.,* **107**(B1), ECV 7-1–ECV 7-8.

Tregoning, P. & Gorbatov, A., 2004. Evidence for active subduction at the New Guinea Trench, *Geophys. Res. Lett.,* **31,** L13608, doi:10.1029/2004GL020190.

Tregoning, P. *et al.*, 1998. Estimation of current plate motions in Papua New Guinea from Global Positioning System observations, *J. geophys. Res.,* **103**(B6), 12 181–12 203.

Tregoning, P., Jackson, R.J., McQueen, H., Lambeck, K., Stevens, C., Little, R.P., Curley, R. & Rosa, R., 1999. Motion of the South Bismarck Plate, Papua New Guinea, *Geophys. Res. Lett.,* **26,** 3517–3520.

Tregoning, P., Burgette, R., McClusky, S.C., Lejeune, S., McQueen, H. & Watson, C.S., 2013. A decade of great earthquake deformation, *J. geophys. Res.,* **118,** 2371–2381.

Wallace, L.M. *et al.*, 2004. GPS and seismological constraints on active tectonics and arc-continent collision in Papua New Guinea: implications for mechanics of microplate rotations in a plate boundary zone, *J. geophys. Res.,* **109,** B05404, doi:10.1029/2003JB002481.

Wallace, L.M. *et al.*, 2014. Continental breakup and UHP rock exhumation in action: GPS results from the Woodlark Rift, Papua New Guinea, *Geochem. Geophys. Geosyst.,* **15,** 4267–4290.

White, L.T., Morse, M.P. & Lister, G.S., 2013. The location of lithospheric-scale transfer faults and their control on the Cu-Au deposits of New Guinea, *Solid Earth Discussions,* **5**(2), 1687–1720.

SUPPORTING INFORMATION

Additional Supporting Information may be found in the online version of this paper:

Figure S1. The rotational and elastic strain rate parts of the modelled velocity field with respect to Australia.
Figure S2. Velocity residuals from the best-fit model (observed minus modelled) and the 95 per cent confidence ellipses.
Figure S3. Velocity residuals from the best-fit model (observed minus modelled) zoomed to the rectangle drawn in Fig. S2 and the 95 per cent confidence ellipses.
Figure S4. Comparison between observed and calculated slip vectors azimuth.
Table S1. Table of east and north GPS velocity components (V_e, V_n) and 1σ uncertainties (σ_e, σ_n) in an Australia-fixed reference.
Table S2. Table of poles of rotation for the modelled blocks relative to Australia (ω, rotation rate; a, semi-major axis of error ellipse; b, semi-minor axis of error ellipse).
Table S3. Summary of F-test distribution results for different models with the best fit model (P, probability that improvement to fit from addition of parameters is not due to chance; Dof, degree of freedom) (http://gji.oxfordjournals.org/lookup/suppl/doi:10.1093/gji/ggv200/-/DC1).

Please note: Oxford University Press is not responsible for the content or functionality of any supporting materials supplied by the authors. Any queries (other than missing material) should be directed to the corresponding author for the paper.